

The work described in this text is published in
Atmospheric Environment 39/18 (2005) 3279-3289

A neural network forecast for daily average PM₁₀ concentrations in Belgium

Hooyberghs Jef ^{*a}, Mensink Clemens^a, Dumont Gerwin^b, Fierens Frans^b, Brasseur Olivier^c

^a*Flemish Institute for Technological Research (VITO), Boeretang 200, B-2400 Mol, Belgium*

^b*Interregional Cell for the Environment (IRCEL), Kunstlaan 10-11, B-1210 Brussels, Belgium*

^c*Royal Meteorological Institute (RMI), Ringlaan 3, B-1180 Brussels, Belgium*

Abstract

Over the past years, the health impact of airborne particulate matter (PM) has become a very topical subject. In the environmental sciences a lot of research effort goes towards the understanding of the PM phenomenon and the ability to forecast ambient PM concentrations. In this paper we describe the development of a neural network tool to forecast the daily average PM₁₀ concentrations in Belgium one day ahead. This research is based upon measurements from ten monitoring sites during the period 1997-2001 and upon ECMWF simulations of meteorological parameters. The most important input variable found was the boundary layer height. A model based on this parameter currently operational online serves to monitor the daily average threshold of 100 µg/m³. By extending the model with other input parameters we were able to increase the performance only slightly. This brings us to the conclusion that day to day fluctuations of PM₁₀ concentrations in Belgian urban areas are to a large extent driven by meteorological conditions and to a lesser extent by changes in anthropogenic sources.

Keywords: particulate matter, prediction, neural networks, boundary layer height, air pollution

* Corresponding author: Jef Hooyberghs, VITO, Boeretang 200, B-2400 Mol, Belgium
jef.hooyberghs@vito.be, fax: +32 (0)14 32 27 95

1. Introduction

The adverse effects of airborne ambient particulate matter have become a well recognised problem in environmental sciences. Besides the reduction of visibility and the deposition of trace elements, the direct impact on human health via inhalation is an important issue. In several studies a significant relation was found between health effects and elevated concentrations of atmospheric PM₁₀ or PM_{2.5} (particulate matter with an aerodynamic diameter below 10 or 2.5 µm): e.g. Dockery et al. (1993), Pope et al. (1995), Pope et al. (2002). Although the health impact is most pronounced for PM_{2.5} and long term exposure, an increased PM₁₀ concentration has been found to result in an increased mortality the day after (e.g. Samet et al., 2000).

Furthermore, for several years PM is of importance as a European policy topic. In order to reduce the health effects of PM₁₀, the EU issued Council Directive 1999/30/EC on 22 April 1999 (European Community 1999). It defines restrictions for the yearly and 24-hour averaged PM₁₀ concentrations for 2005 and 2010.

This paper concerns the ground level atmospheric PM₁₀ concentrations in the central West European country of Belgium. These have been measured since 1996 in the telemetric air quality networks of the three Belgian regions. Currently 41 PM-monitoring sites are operated using both β-attenuation instruments and tapered element oscillating microbalances.¹ In the Brussels-Capital Region, the concentration level for warning the public in case of increasing exposure to PM₁₀ is set at a daily average of 50 µg/m³. The concentration level at which the public is to be alarmed is set at 100 µg/m³. In case of a foreseen exceedance, a special warning bulletin is to be issued by the Belgian Interregional Cell for the Environment (IRCEL-CELINE). One of the tools currently used for this forecast is the model described in this paper, which is based on a neural network methodology.

(Artificial) neural networks (NN) form a group of machine learning techniques that are inspired by biological neurons. Their history goes back more than 50 years, but due to the availability of modern computers from the 1980's they have grown to be a competitive tool that has been applied widely since the mid 1990's. One of the reasons for their success is their capability to make regressive approximations of **non-linear** functions in **high-dimensional** spaces, something that is missing in classical statistics. The flexibility of NN's has led to their

¹ To be compatible with the EU referential technique (gravitational method) a correction factor is used: respectively 1.37 and 1.47.

use in all possible scientific branches. An overview of some applications in the atmospheric sciences during the 1990's can be found in Gardner and Dorling (1998). In this article references can be found to successful applications of NN's in predicting ambient concentrations of air pollutants like e.g. ozone, sulphur dioxide and carbon monoxide. The main advantages of a NN forecasting tool, compared to deterministic atmospheric modelling systems, are the limited need for input data and computer power (in operational mode, training can of course be computer intensive). Compared to traditional statistical techniques a NN excels by its flexibility. The main drawback is that a NN which is trained by data from a given measuring location can only forecast for that specific location and it cannot give insight into the physics behind the data: a NN merely learns from examples and it is not suited to generalise to other situations.

Recently, several researchers started to use the NN techniques to forecast airborne particulate matter concentrations: e.g. Perez and Reyes (2002), Lu et al. (2003), Kukkonen et al. (2003), Ordieres et al. (2004). They conclude that a NN can be a useful tool to predict PM, although the accuracy they could reach is limited (e.g. lower than that for NO₂: Lu et al. (2003), Kukkonen et al. (2003)). No reference was made by any of these authors to the use of such a model in an operational PM forecasting system yet.

In this paper we describe the design of a NN forecasting tool for the ambient PM₁₀ concentrations in Belgium. In the following section we first state our objectives and describe the available resources. In section 3 the methodology of our research is outlined and the results are analysed in section 4. In the final section we make a summary and state our conclusions.

2. Objectives and resources

To state our objectives clearly we first define some abbreviations that will be used:

day0:	the day on which the forecast is made
dayN:	days relative to day0 (N = ..., -1, 0, 1, ...)
<...> _{dayN} :	daily average of a quantity on dayN.
<...> _{dayN,1-9h} :	average of first 9 hours of dayN.

The goal is to develop a forecasting model for the daily average PM_{10} ; at noon of day0 the model is developed to predict the ground level values $\langle PM_{10} \rangle_{\text{day}N}$ for $N = 0, 1, 2$ that will be measured at the different monitoring sites. The emphasis is on high PM_{10} values, typically above $100\mu\text{g}/\text{m}^3$, since it will be used in triggering a warning bulletin. The model should be simple and fast, i.e. it is not our intention to design a simulation model but rather an algorithm that on a statistical basis can relate future PM_{10} values to a set of available input variables. Since the design of a forecast model for dayN is in principle the same for all N, we will restrict the discussion in this paper to the most relevant case $N = 1$: forecast for tomorrow.

Concerning the resources, the required input data for our purpose is twofold:

input parameters:

- initial conditions: variables **measured** before noon of day0
 - future conditions: **forecasted** meteorological variables.
- (1)

For the development of a representative model, a detailed and large dataset for these quantities is vital. The restrictive part of such a set is usually the available PM_{10} data. In this research, from the 41 active PM_{10} measuring stations in Belgium, we retain the ten with the longest history: the dataset consists of half-hourly values and covers the period 1997-2001. For these years we also use analyzed meteorological simulation data by ECMWF with a temporal resolution of 6 hours and a spatial resolution of 0.5 degrees. From this dataset we will now try to select features that carry useful information for the prediction of PM_{10} concentrations.

The precise location of the monitoring sites is given in Figure 1 together with a further classification: background, traffic or industrial; all sites are non-rural.

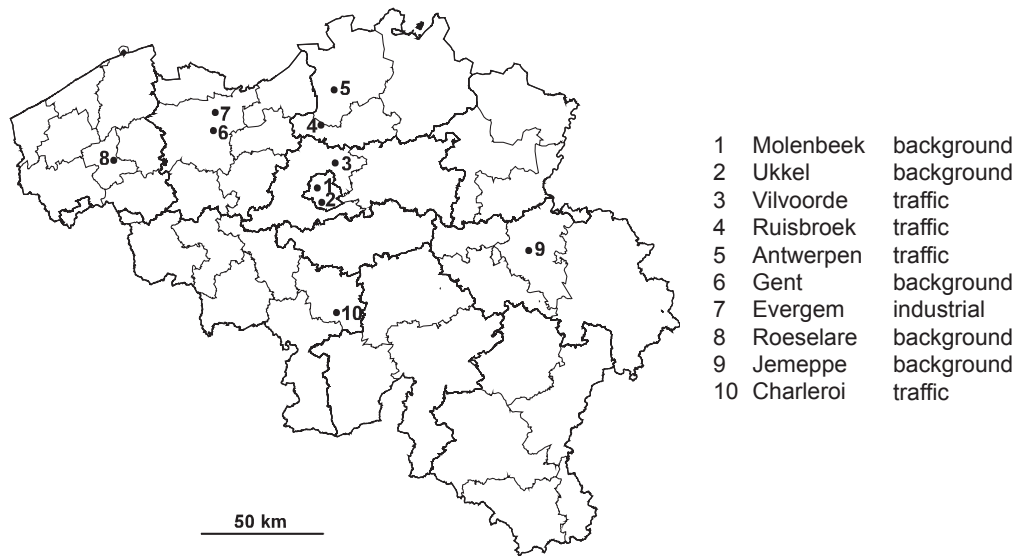


Fig. 1. Location and identification number of PM_{10} monitoring stations used in this paper.

3. Methodology

3.1 Neural network approach

The problem we are faced with could be called a regression problem. On the basis of a set of known input variables (1) we have to produce an output variable that is on average a good estimate for the target $\langle PM_{10} \rangle_{day1}$. This implies the design of a model that can fit the relation between the input - and target parameters on the basis of an historical dataset. Since the input space is multidimensional and the functional relation with the target is a priori unknown and most likely non-linear, traditional parametric regression techniques are not well suited. For this job a neural network approach is more appropriate. In the rest of this subsection we briefly describe our methodology, but for a more profound introduction to the NN techniques see Bishop (1995).

For each monitoring site a NN has to be designed to fit a function between the chosen inputs and the target $\langle PM_{10} \rangle_{day1}$. From historical data one constructs a collection of records, consisting of the input vector and the corresponding target. Next, a part of the dataset is used for the training of the neural network: the non-linear curve fitting. The rest of the dataset usually serves as an independent test set by which the (generalisation)

performance of the NN is validated. The dataset used in our research covers the years 1997 to 2001. Four of these years were used for the training. The fifth year was used as an independent test set. We repeated this calculation 5 times, once for each test year, resulting in a large test set from which we could deduce in a reliable way the accuracy of the forecasting model.

Since episodes of high PM concentrations are not that frequent (in the considered sites daily average concentrations above $100 \mu\text{g}/\text{m}^3$ are measured on about 5 to 10 days per year), an historical data set contains more low than high PM₁₀ targets. We are however, particularly interested in predicting high PM₁₀ concentrations, therefore we constructed our training set by resampling from the four-year dataset. We put equal emphasis on all targets, by drawing records from the data set and collecting them in a training set in such a way that all observed PM₁₀ values are represented with the same probability. This has the advantage of improving the prediction precision for high concentrations. The drawback is that the residual error is biased, therefore we did not perform this resampling in the construction of the residual scatter plots of Figure 2c)d).

For the NN we chose the following technical setup. We used the feed-forward multi-layer perceptron with one hidden layer of four nodes. The sum-of-squares error was minimised by the resilient back-propagation algorithm. To avoid overtraining we applied regularisation, which was optimised by cross-validation.

3.2 Discussion and selection of input variables

A crucial step in the development of a forecast model is the choice of input parameters (1). In principle, any set can be fed into the NN for training and evaluation. However, the number of possible parameters and the number of ways they can be presented, is too high to test all possible combinations. We have to restrict ourselves to a limited number of tests, based on the available experience and knowledge of the PM₁₀ phenomenon.

It is known that the temporal and spatial variations of PM concentrations are governed by a complex interplay of many parameters (e.g. Harrison and Van Grieken, 1999). Atmospheric particulates can be both of primary or secondary origin. The primary particulates are mainly emitted by anthropogenic sources like mechanical friction, smelting or combustion of fossil fuels, but also natural phenomena like wildfires can emit PM. Secondary particulates originate from chemical reactions, condensation and coagulation in the atmosphere. This formation is influenced by concentrations of other atmospheric pollutants and by meteorological

conditions like humidity and solar radiation. The amount of atmospheric PM is further determined by deposition and transport by winds. But even when the total amount of PM₁₀ above a given location is known, the ground level concentration is still uncertain if the vertical concentration profile is unknown. Hence, the (in)stability of the atmospheric state can be of major importance. This will be confirmed in this paper and can also be found in other articles like e.g. Termonia and Quinet (2004).

Table 1

Description of input parameters for prediction of $\langle PM_{10} \rangle_{day1}$

parameter	description
$\langle PM_{10} \rangle_{day0,1-9h}$	average PM ₁₀ concentration, measured during first 9 hours of day0
$\langle BLH \rangle_{day1}$	day1 average of boundary layer height (ECMWF prediction of height where bulk Richardson number equals 0.5)
$\langle windspd \rangle_{day1}$	day1 average of wind speed (ECMWF prediction of wind speed at 10 m height)
$\langle temp \rangle_{day1}$	day1 average of temperature (ECMWF prediction of temperature at 2 m height)
$\langle cloud \rangle_{day1}$	day1 average of cloud cover (ECMWF prediction of medium height cloud cover)
$\langle winddir \rangle_{day1}$	day1 average of wind direction (ECMWF prediction wind direction at 10 m height)
DOW	day of week of day1

In Table 1 we list the input parameters that we will examine for the prediction of $\langle PM_{10} \rangle_{day1}$. First of all we have the PM₁₀ concentrations that are measured in the relevant monitoring site during the morning of day0. They characterise the PM₁₀ situation at the moment the forecast is made. We chose an average of the first 9 hours because this is long enough to contain the morning traffic peak and not too close to noon to ensure availability of the measurements in operational mode. The second parameter is the predicted boundary layer height. This BLH is defined as the height above which the atmospheric bulk Richardson number (Ri) exceeds 0.5; for a detailed definition see e.g. Vogelezang and Holtslag (1996). Ri is the ratio between the buoyancy force (determined by the vertical temperature profile) and the inertia force (determined by the turbulence of the air). If Ri is sufficiently small (or even negative for an unstable temperature profile) the turbulence is strong enough to carry particulates in the vertical direction against a possibly stabilising temperature profile. Hence

the BLH is a measure for the height up to which particulates can spread due to turbulence in the lower troposphere. This BLH is always well defined (both in a stable and an unstable lower atmosphere), which is an important property for an input of a NN. In a previous study the BLH was already identified as a significant indicator for PM_{10} concentrations in Belgium (Hooyberghs et al. 2004). Next we have the wind speed which is closely related to the amount of air- and hence PM transport. The cloud cover at medium height and the temperature are used because they influence the formation of secondary PM_{10} . We do not discuss the cloud cover at small or large heights: from a simple scatter plot like Figure 2a)b) (explained in the next paragraph) they turned out to be inferior to the medium height cloud cover. Finally the wind direction and day of the week are considered, since they can be of importance when the PM_{10} emissions are non-homogeneous in space or time.

Before we turn to the NNs, it is instructive to take a look at the data itself. First of all, the probability to find a certain PM_{10} concentration at a given moment has a distribution that resembles a lognormal distribution. Therefore we will consider here the logarithmic PM_{10} values, which consequently have a Gaussian-like distribution. Next we make scatter plots of the input parameters versus the logarithm of the target $\langle PM_{10} \rangle_{day1}$ as in the figures 2a). Since the latter has a Gaussian-like distribution, we use its mean and standard deviation to normalise it to a standard normal. Now, if an input parameter has any explanatory value with respect to PM_{10} , the data points of that scatter plot should follow with a certain precision a functional relation with a non-zero slope. As a guide to the eye we add the figures 2b): the X-axis is divided in a number of bins in which we calculate the mean and standard deviation of the Y-values. In figures 2b) these means \pm std are plotted versus the X-values of the bin centres. This gives a better visualisation of the tendency in the bulk of the data points; at the border of the data cloud however, it is less correct. From figures 2a)b) one can now get a first impression of the relative importance of the different input parameters. All parameters contain some explanatory value, but not all with the same magnitude.

As a starting point we will now discuss a forecast model based upon only two input parameters: one describing the initial condition and one the future condition (cf. (1) and Table 1). For the initial condition we will obviously use $\langle PM_{10} \rangle_{day0,1-9h}$, which also seems promising from Figure 2. From the parameters for the future condition, one finds in Figure 2 that the $\langle BLH \rangle_{day1}$ has the most pronounced slope for the bulk of the data points. Since this was the case for all monitoring sites (Figure 1), $\langle BLH \rangle_{day1}$ will be used as the second input parameter. Later we will try to improve this model by including extra parameters. In the current analysis we use analysed meteorological simulation data, however in operational the ECMWF run of 00 UT is used.

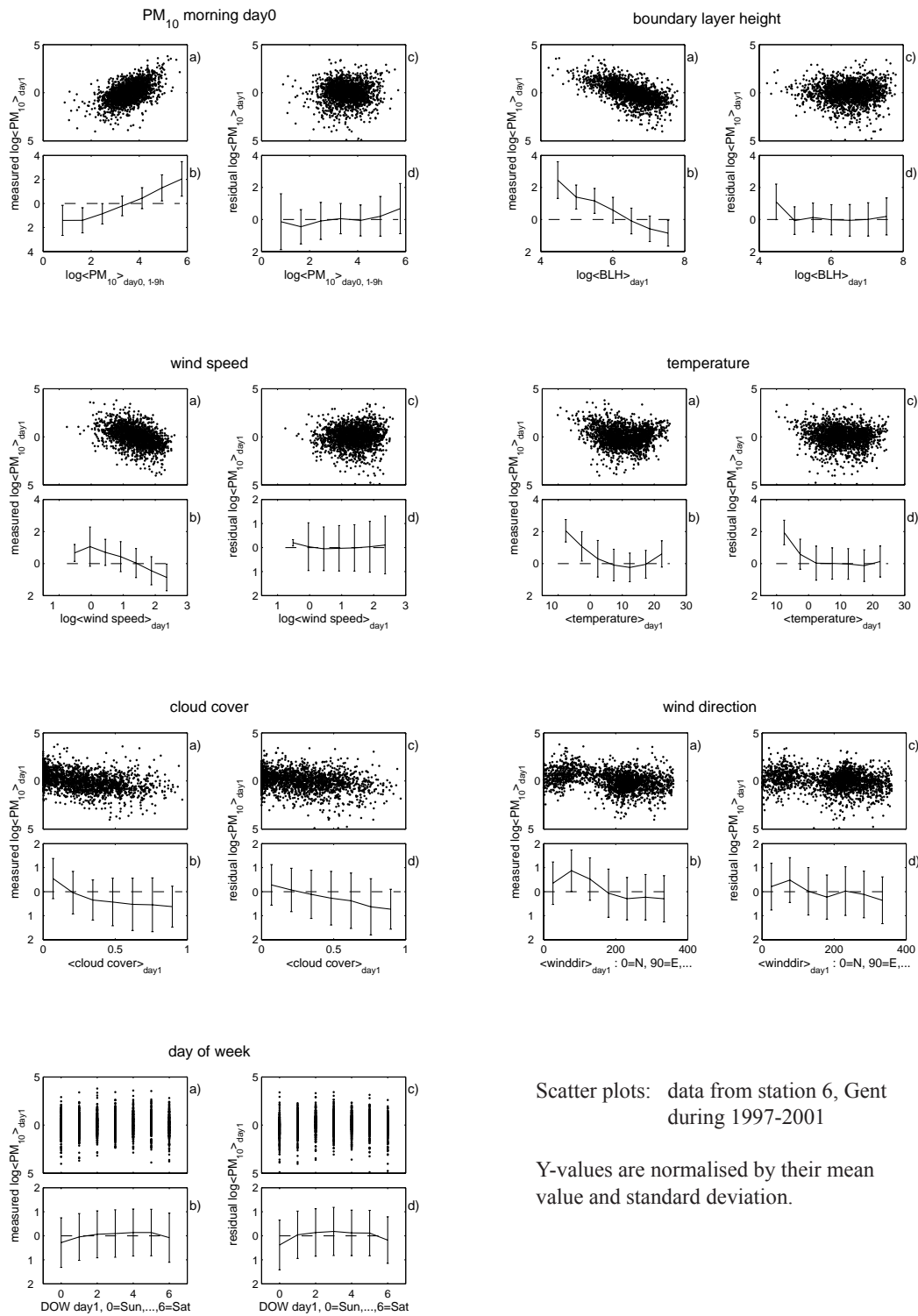


Fig. 2. Input parameters versus:

- a) logarithm of the target: measured $\langle \text{PM}_{10} \rangle_{\text{day1}}$
- b) x-axis of a) is divided in bins, the mean \pm std of y-values are plotted per bin
- c) residual = log of target $\langle \text{PM}_{10} \rangle_{\text{day1}}$ – log of model 1 forecasted $\langle \text{PM}_{10} \rangle_{\text{day1}}$
- d) x-axis of c) is divided in bins, the mean \pm std of y-values are plotted per bin

4. Results

4.1 Quality indicators

Before we construct and compare different models, we have to specify how the forecast errors will be quantified. In our case the aim is twofold. In the first place we want an accurate prediction for the whole range of observable $\langle \text{PM}_{10} \rangle_{\text{day1}}$ concentrations. Hence, as a first quality indicator we use the **root-mean-square error RMSE**, which gives a global and absolute error in units of $\mu\text{g}/\text{m}^3$. It is also sensible to weight this error by the standard deviation of the observed values. This is done by using the **correlation coefficient R** between the observed and forecasted values. RMSE and R can be calculated for each monitoring site separately; the better the forecast, the smaller RMSE and the closer R is to 1. On the other hand, the predictions are meant to trigger a warning mechanism. For this purpose, the model should be able to predict (non)-exceedances of a threshold concentration. To be more precise, we want to discriminate between a PM₁₀day/non-PM₁₀day: a day on which *at least one/none* observation station will measure a daily average PM₁₀ concentration above a given threshold. To quantify the ability of the model to make this classification, we use the **success index SI**. Denote an observed (non-)PM₁₀day by O (O'), and a forecasted one by F (F'). We can now write e.g. the number of days that a PM₁₀day was observed, while a non-PM₁₀day was forecasted by $N(O, F')$. With this notation, the SI is defined as

$$SI = \left[\frac{N(O, F)}{N(O, F) + N(O, F')} + \frac{N(O', F')}{N(O', F') + N(O', F)} - 1 \right] 100. \quad (2)$$

The SI gives one value for the whole set of monitoring sites and is only defined with respect to a given threshold concentration. The index is a combination of the skill of forecasting threshold exceedances and non-exceedances, it has a value between -100 (worst classification) and +100 (perfect classification).

4.2 Model 1

We now examine the first NN model, defined in (3).

Model 1:

$$\begin{aligned} \text{2 input parameters:} & \quad \langle \text{PM}_{10} \rangle_{\text{day0}, 1-9\text{h}} \quad (\text{measurement}) \\ & \quad \langle \text{BLH} \rangle_{\text{day1}} \quad (\text{weather forecast}) \\ \text{target:} & \quad \langle \text{PM}_{10} \rangle_{\text{day1}}. \end{aligned} \tag{3}$$

As mentioned at the end of section 3, we only use two input parameters: the average PM_{10} concentration of the first 9 hours of day0, and the forecasted day1 average of the boundary layer height. For each monitoring site we train a NN (cf. Appendix) and subsequently make an evaluation of the NN forecast precision.

The performance of this NN, which we will call model 1, is summarised in Figure 3: the first two plots show the R and RMSE for every monitoring station², while the last plot shows the SI of the whole set of stations as a function of a given threshold. To make a comparison possible, we include the persistence model: the pollution is assumed to remain constant and the PM_{10} concentration of tomorrow is simply set equal to that of yesterday. The essence of Figure 3 is prominent: model 1 outperforms the persistence model significantly on all three evaluation quantities. The effect is most pronounced for the success index at high threshold concentrations. Exceedances of a high threshold can be seen as rare events that do not last for long and consequently can not be foreseen by a simple persistence model. Model 1 however, does get a fair score for this classifying task.

² Note that the lines between the stations are meaningless, they are only there for sake of visibility.

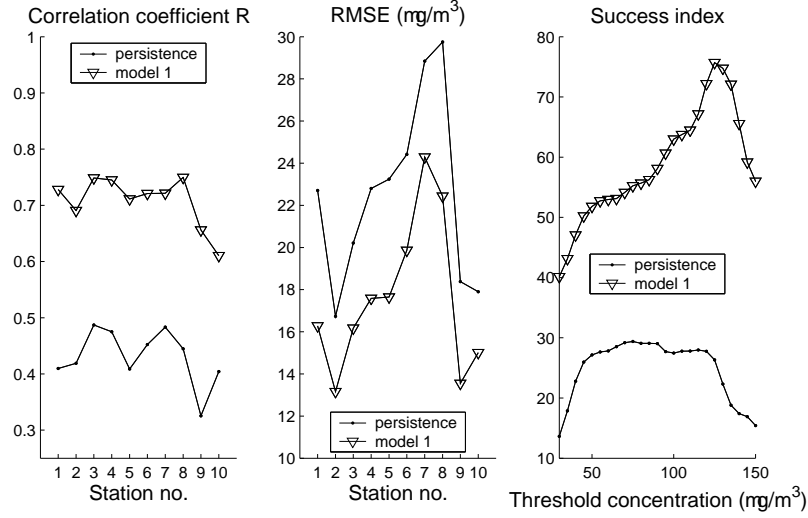


Fig. 3. Forecast results for PM_{10} average of day1 produced by model 1 and the persistence model, visualised by three evaluation quantities.

The BLH of model 1 quantifies the mixing state of the lower troposphere, it does not contain information on the amount of PM- or precursor emissions neither does it have a direct link with horizontal PM transport or the formation of secondary PM_{10} . Therefore, an evaluation of the other input parameters from Table 1 seems desirable.

4.3 Model 2: extra inputs

Since the BLH is clearly an important input parameter, we will retain this parameter and evaluate another one by adding it to the set of inputs and compare the resulting NN model with model 1. However, before we do this, it is again instructive to look at the data. In Figure 2c)d) we plot the residual (4) of model 1 versus the input parameters.

$$\text{Residue} = \log\left(\text{measured } \langle PM_{10} \rangle_{\text{day1}}\right) - \log\left(\text{forecasted } \langle PM_{10} \rangle_{\text{day1}}\right) \quad (4)$$

Since the residual, like PM_{10} itself, has a Gaussian-like distribution we normalise it in Figure 2 to a standard normal. This has the important advantage that a comparison is possible between Figure 2a)b), which shows the

explanatory value of an input with respect to PM_{10} , and Figure 2c)d), which shows the explanatory value **complementary to model 1**. (Figure 2 only shows the situation for the monitoring site in Gent, but the plots of the other Belgian stations show the same behaviour.)

For the two inputs of model 1, $\langle PM_{10} \rangle_{\text{day0, 1-9h}}$ & $\langle BLH \rangle_{\text{day1}}$, the conclusion is obvious and clear: they have a high explanatory value, but none complementary to model 1. (This merely states that the NN of model 1 successfully learned to use the information contained within these input parameters.) Figure 2 shows however, that the same is true for the wind speed. All useful information of the wind speed is clearly also contained within the BLH. To a large extent the same story holds for the temperature where the bulk of the data points of Figure 2b)c) follows a line with zero slope. This indicates that the BLH alone contains a lot of the relevant meteorological information. For the cloud cover and the day of the week, the situation is different: their explanatory value seems to be complementary to model 1. The cloud cover gives a nice monotonous relationship with the residual, while for the day of the week an over/under estimation by model 1 is noticeable during the weekends/week. For the wind direction the situation is somewhat complicated. In Figure 2a)b) one notices that easterly winds are more often accompanied by high PM_{10} concentrations than westerly winds. This seems reasonable since Belgium lies between the North Sea on the west and the European continent with a lot of industry to the east, so westerly winds contain less PM than easterly. Figure 2c)d) shows however that this is only a partial explanation: the explanatory value of the wind direction is reduced when evaluated on the residual of model 1. This suggests that a part of the east-west PM_{10} contrast is due purely to BLH conditions. Indeed, in Belgium the BLH is on average lower on days with easterly winds, consequently it is not only the high total amount of PM_{10} in the troposphere that explains the high ambient PM_{10} values, but also the limited vertical distribution of particulates.

In order to check and quantify the conclusions based on the residual plots of Figure 2, we proceed with the NN approach. We add each of the five extra inputs to model 1, train and evaluate the NN as described in the Appendix and Section 4.1. The results are shown in Figure 4; they confirm the previous evaluation. The wind speed and temperature contain little complementary information. When they are used in the model, a larger NN has to be trained with very little extra information, resulting in a reduction of the forecast precision. Day of the week and especially cloud cover do contain complementary explanatory value and improve the NN

performance. The wind direction is somewhat ambiguous. For some monitoring sites it gives improvement for some it doesn't.

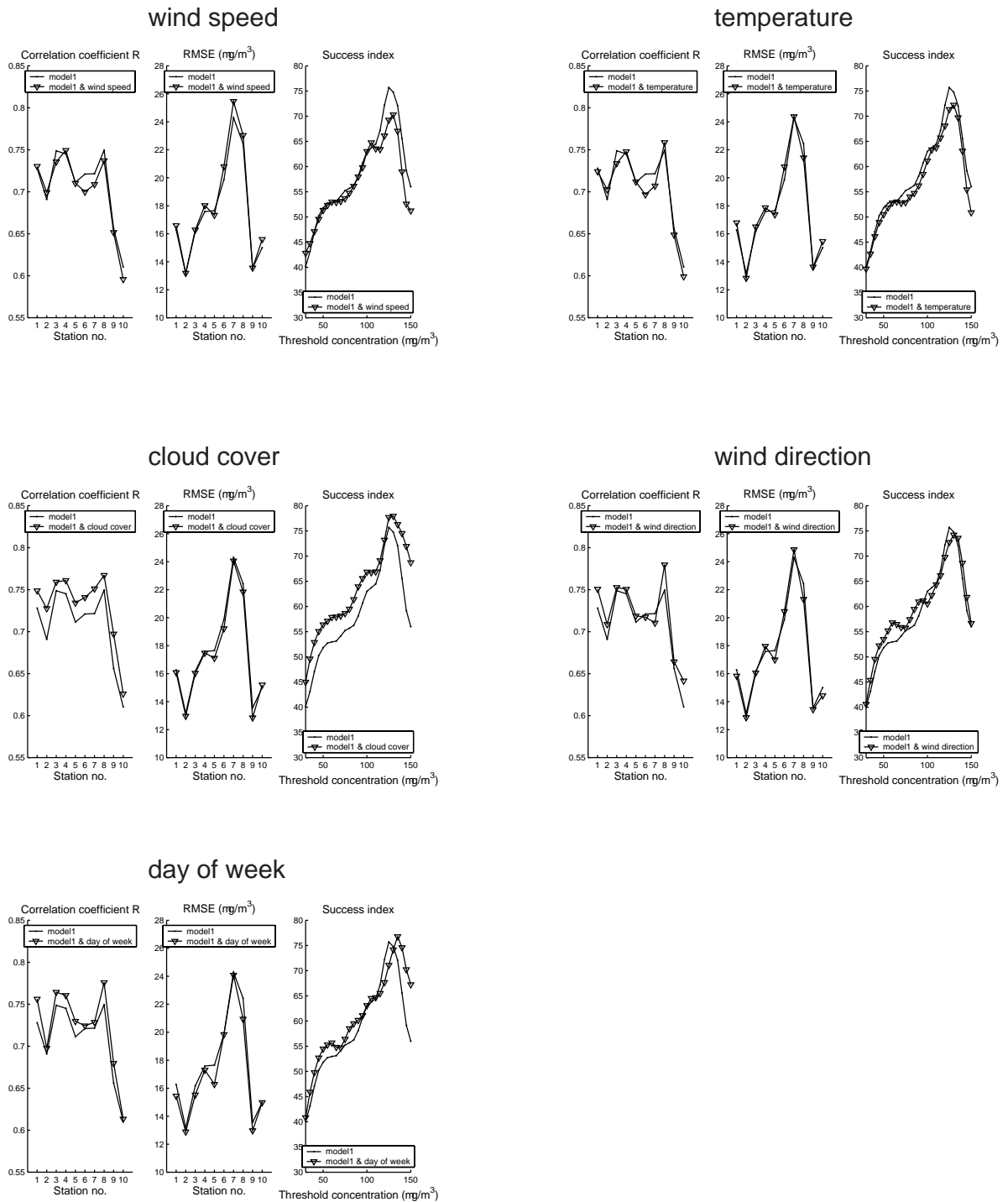


Fig. 4. Forecast results for PM_{10} average of day1, visualised by three evaluation quantities, and produced by model 1 and model 1 with one extra input parameter.

Furthermore, from these NN results it becomes clear that the forecast improvements to model 1 induced by some of these parameters are small compared with that of model 1 to the persistence model. This is clearly illustrated in Figure 5. Here we compare the persistence model with model 1 and model 2, the latter is defined in (5) and makes use of all five constructive input parameters.

Model 2:

$$\begin{aligned}
 \text{5 input parameters:} \quad & \langle \text{PM}_{10} \rangle_{\text{day0, 1-9h}} && \text{(measurement)} \\
 & \langle \text{BLH} \rangle_{\text{day1}}, \langle \text{cloud} \rangle_{\text{day1}}, \langle \text{winddir} \rangle_{\text{day1}} && \text{(weather forecast)} \\
 & \text{day of week of day1} \\
 \text{target:} \quad & \langle \text{PM}_{10} \rangle_{\text{day1}}. && (5)
 \end{aligned}$$

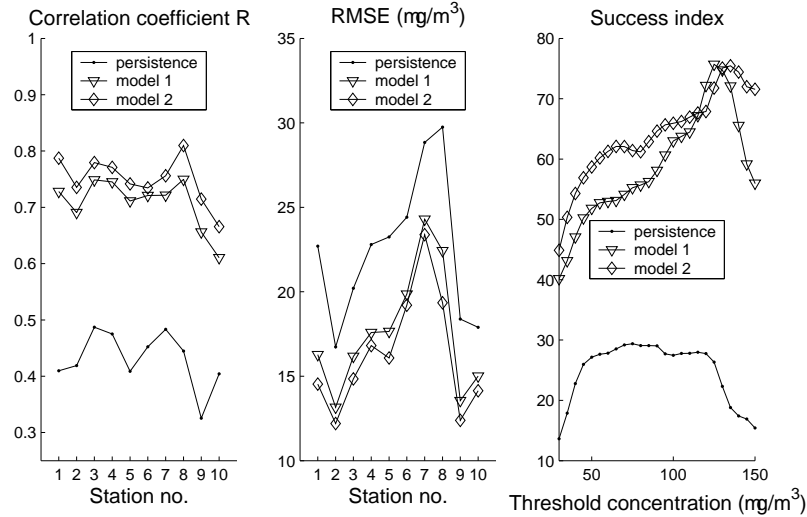


Fig. 5. Forecast results for PM_{10} average of day1, visualised by three evaluation quantities, and produced by the persistence model, model 1 and model 2.

As a final analysis we present Table 2. Here some performance quantities are evaluated with respect to the relevant (high) threshold of 100 $\mu\text{g}/\text{m}^3$.

Table 2

Forecast of exceedances of 100 $\mu\text{g}/\text{m}^3$ threshold (PM_{10} average of day1).

		Model 2	Model1	Persistence
FCF:	Fraction of correctly forecasted exceedances	73 %	70 %	33 %
FRF:	Fraction of realised forecasted exceedances	46 %	46 %	33 %
SI:	Success index	66	63	27

The success index was already defined in (2) from section 4.1. Using the same notation, we now define:

$$\begin{aligned}
 FCF &= \frac{N(O, F)}{N(O, F) + N(O, F')} \cdot 100\% = \frac{N(O, F)}{N(O)} \cdot 100\% \\
 FRF &= \frac{N(O, F)}{N(O, F) + N(O', F)} \cdot 100\% = \frac{N(O, F)}{N(F)} \cdot 100\%
 \end{aligned} \tag{6}$$

where $N(O)$ and $N(F)$ are respectively the number of observed and forecasted PM_{10} days.

If the number of days is large enough, we can make the following interpretation: FCF is the probability that the model forecasts an exceedance of 100 $\mu\text{g}/\text{m}^3$ given that an exceedance will be observed; FRF is the probability that an exceedance will be observed given that the model forecasts one. Table 2 shows that the major improvement occurs from the persistence model to model 1.

5. Discussion and conclusions

5.1 The PM₁₀ phenomenon in Belgium

Now that we have selected and compared the relevant features for the prediction of ambient particulate matter, we can try to use this knowledge to further analyse the behaviour of PM₁₀ concentrations in Belgium. We have to be careful however. When a certain input parameter increases the accuracy of the neural network forecast, it is right to consider this a relevant feature (even though this does not imply any causal relation), but the opposite is not always justified. When a new input does not increase the forecast accuracy, in principle this merely means that the neural network is unable to draw useful information from it: one can never be completely conclusive about the absence of useful information. However, in this research the effect of an input on the neural network performance (Figure 4) was always found to be consistent with the visible information in the scatter plots of the data (Figure 2).

If we now reconsider Figure 2, Figure 5 and Table 2 it is clear that the most important parameter is by far the boundary layer height. If we compare model 1 with the persistence model we can say that the BLH can explain a large fraction of the short term fluctuations in PM₁₀ daily averages. This is somewhat surprising since this parameter does not contain information on inhomogeneities in space of transport nor in time or space of emissions. The BLH is merely a measure for the height up to which turbulence can carry particulates. Moreover, if we include parameters that describe these inhomogeneities (wind direction, day of week) the increase of forecast accuracy is only minor. Besides the BLH, the second most significant parameter turned out to be the medium height cloud cover.

A study as this can never be conclusive, but we have the impression that short term fluctuations of daily PM₁₀ concentrations in the studied Belgian monitoring sites are to a large extent driven by meteorological conditions and to a lesser extent by changes in anthropogenic sources.

5.2 Conclusions

The goal of this research was to examine the feasibility of a statistical short term forecasting model for ambient PM₁₀ concentrations in Belgium, as stated in section 2. The emphasis is on high concentrations with an explicit interest on the threshold of 100 µg/m³. We started with model 1, which is a neural network that uses two input parameters: the forecasted boundary layer height and the PM₁₀ measurements of the morning of day0: cf. (3). This model has a reasonable accuracy and is currently tested in online operational mode (IRCEL-CELINE). In the previous section, three parameters were found to increase the forecast accuracy when added to model 1: cloud cover, day of week and wind direction. These parameters contain explanatory value for the PM₁₀ phenomenon in Belgium, complementary to the two inputs of model 1. On the other hand, we were not able to gain additional accuracy from the use of temperature or the wind speed. All the positively evaluated parameters were collected to form the input set of model 2: cf. (5). The forecast results for day1 are summarised in Figure 5, in which one finds an increase of precision from the persistence model to model 1 to model 2. From FCF and FRF in Table 2, one finds for the 100 µg/m³ threshold that around three out of four exceedances are predicted by model 2, while a predicted exceedance has roughly a one out of two chance of actually occurring.

In Belgium, all input variables of model 2 are nowadays readily available from measurements or weather forecast, hence model 2 can be implemented as an operational PM₁₀ forecast module.

References

- Bishop, C.M., 1995. *Neural Networks for Pattern Recognition*, Oxford University Press: Oxford.
- Dockery, D.W., Pope, C.A. III, Xiping, X., Spengler, J.D., Ware, J.H., Fay, M.A., Ferries, B.G. Jr., Speizer, F.E., 1993. An association between air pollution and mortality in six US cities. *The New England Journal of Medicine* 329(24), 1753-1759.
- European Community 1999, Council Directive 1999/30/EC of 22 April 1999 relating to limit values for sulphur dioxide, nitrogen dioxide and oxides of nitrogen, particulate matter and lead in ambient air. *Official Journal of the European Communities*, L 163, 0041 – 0060.
- Gardner, M.W., Dorling, S.R., 1998. Artificial neural networks (the multilayer perceptron)- a review of applications in the atmospheric sciences. *Atmospheric Environment* 32, 2627-2636.

Harrison, R.M., Van Grieken, R., 1999. Atmospheric Particles, IUPAC Series on Analytical and Physical Chemistry of Environmental Systems, Vol. 5, (Series Eds. Jaques Buffle and Herman P Van Leeuwen) John Wiley & Sons.

Hooyberghs, J., Mensink, C., Dumont, G., Fierens, F., Brasseur, O., 2004. Short term PM₁₀ forecasting: a survey of possible input variables. Air Pollution XII, Series: Advances in Air Pollution, Vol. 14, (Ed. C.A. Brebbia) WIT Press, 171-178.

IRCEL-CELINE website: <http://www.irceline.be>

Kukkonen, J., Partanen, L., Karppinen, A., Ruuskanen, J., Junninen, H., Kolehmainen, M., Niska, H., Dorling, S., Chatterton, T., Foxall, R., Cawley, G., 2003. Extensive evaluation of neural network models for the prediction of NO₂ and PM₁₀ concentrations, compared with a deterministic modelling system and measurements in central Helsinki. Atmospheric Environment 37, 4539-4550.

Lu, W.Z., Wang, W.J., Wang, X.K., Xu, Z.B., Leung, Y.T., 2003. Using improved neural network model to analyse RSP, NO_x and NO₂ levels in urban air in Mong Kok, Hong Kong. Environmental Monitoring and Assessment 87, 235-254.

Ordieres, J.B., Vergara, E.P., Capuz, R.S., Salazar, R.E., 2004. Neural network prediction model for fine particulate matter (PM_{2.5}) on the US–Mexico border in El Paso (Texas) and Ciudad Juárez (Chihuahua). Environmental Modelling & Software, In press.

Perez, P., Reyes, J., 2002. Prediction of maximum of 24-h average of PM₁₀ concentrations 30 h in advance in Santiago, Chile. Atmospheric Environment 36, 4555-4561.

Pope, C.A. III, Thun, M.J., Namboodiri, M.M., Dockery, D.W., Evans, J.S., Speizer, F.E., Heath, C.W. Jr., 1995. Particulate air pollution as predictor of mortality in a prospective study of US adults. American Journal of Respiratory and Critical Care Medicine 151, 669-674.

Pope, C.A., Burnett, R., Thun, M.J., Calle, E.E., Krewskik, D., Ito, K., Thurston, G.D., 2002. Lung cancer, cardiopulmonary mortality, and long term exposure to fine particulate air pollution. Journal of the American Medical Association 287, 1132-1141.

Samet, J.M., Zeger, S.L., Dominici, F., Curriero, F., Coursac, I., Dockery, D.W., Schwartz, J., Zanobetti, A., 2000. The National Morbidity, Mortality, and Air Pollution Study. Part II: Morbidity, Mortality and Air Pollution in the United States. Health Effects Institute Research Report 94; Part II. Boston US.

Termonia, P., Quinet, A., 2004. A new transport index for predicting episodes of extreme air pollution. Journal of Applied Meteorology 43 (4), 631-640.

Vogelezang, D.H.P., Holtslag, A.A.M., 1996. Evaluation and model impacts of alternative boundary-layer heights. Boundary-Layer Meteorology 81, 245-269.